Journal of the American Heart Association

ORIGINAL RESEARCH

Nonthermal Irreversible Electroporation to the Esophagus: Evaluation of Acute and Long-Term Pathological Effects in a Rabbit Model

Yue Song, MD; Jingjing Zheng, PhD; Lianhui Fan, MD

BACKGROUND: Esophageal ulceration and fistula are severe complications of pulmonary vein isolation using thermal ablation. Nonthermal irreversible electroporation (NTIRE) is a promising new technology for pulmonary vein isolation in patients with atrial fibrillation. NTIRE ablation technology has been used to treat atrial fibrillation; however, the effects of NTIRE on esophageal tissue have not been clearly described.

METHODS AND RESULTS: A typical NTIRE electrical protocol was directly applied to esophagi in 84 New Zealand rabbits. Finite element modeling and histological analysis with 120 slices were used to analyze electric field intensity distribution and subsequent tissue changes. A parameter combination of 2000 V/cm multiplied by 90 pulses output is determined to be an effective ablation parameters combination. Within 16 weeks after ablation, no obvious lumen stenosis, epithelial erythema, erosion, ulcer, or fistula was observed in the esophageal tissue. NTIRE effectively results in esophageal cell ablation to death, and subsequently, signs of recovery gradually appear: creeping replacement and regeneration of epithelial basal cells, repair and regeneration of muscle cells, structural remodeling of the muscle layer, and finally the restoration of clear anatomical structures in all layers.

CONCLUSIONS: Monophasic, bipolar NTIRE delivered using plate electrodes in a novel esophageal injury model demonstrates no histopathologic changes to the esophagus at 16 weeks. Data of this study suggest that electroporation ablation is a safe modality for pulsed electroporation ablation near the esophagus.

Key Words: ablation ■ esophagus ■ irreversible electroporation ■ tissue regeneration

Atrial fibrillation is the most common arrhythmia. Thermal ablation methods may cause collateral damage to extracardiac structures. Atrial fibrillation has become a fundamental public health problem and is a risk factor for severe comorbidities such as stroke and dementia.[1,2] The traditional thermal techniques used to treat atrial fibrillation include radiofrequency catheter ablation and balloon cryoablation.[3] Performing thermal ablation has been reported to potentially cause protein denaturation and tissue coagulation necrosis, and various manifestations of esophageal damage, such as esophageal ulceration, stricture, and atrial-to-esophageal fistula.[4–6] Therefore, more optimized solutions are then required.

In recent years, nonthermal irreversible electroporation (NTIRE) has been considered to be a promising ablation tool with several potential advantages compared with thermal ablation. NTIRE is an advanced new technology that induces cell death by creating permanent nanopores in the cellular membrane via the application of short intervals of high-voltage direct electrical current.[7] It increases

Correspondence to: Jingjing Zheng, Department of Anesthesia, General Hospital of Northern Theater Command, No. 83, Wenhua Rd, Shenhe District, Shenyang, 110000, China. E-mail: jjzheng_fmmu@163.comand Lianhui Fan, Department of Urology, General Hospital of Northern Theater Command, No. 83, Wenhua Rd, Shenyang, 110000, China. E-mail: fanlianhui1968@163.com

For Sources of Funding and Disclosures, see page 12.

JAHA is available at: www.ahajournals.org/journal/jaha

CLINICAL PERSPECTIVE

What Is New?

- The ability of nonthermal irreversible electroporation to preserve the extracellular matrix, important blood vessels, and nerve bundles allows for a quick recovery of the esophagus after electroporation ablation, and provides an important guarantee for the recovery of peristalsis and secretion of the esophagus.
- Monophasic, bipolar nonthermal irreversible electroporation delivered using plate electrodes in a novel esophageal injury model demonstrates no histopathologic changes to the esophagus. Electroporation ablation is a safe modality for pulsed electroporation ablation near the esophagus.

What Are the Clinical Implications?

- This study constructs a transition bridge from experimental research to clinical application and establishes a safety guarantee for paraesophageal electroporation.

Nonstandard Abbreviations and Acronyms

ECM	extracellular matrix
NTIRE	nonthermal irreversible electroporation
ROI	regions of interest

therapeutic effects while avoiding thermal effects.[8] Catheter-based pulsed field ablation has recently been shown, in preclinical and clinical studies, to effectively ablate atrial and pulmonary venous tissue with remarkable efficacy and safety.[9–13] This has led to its rapid development as an attractive alternative to traditional energy sources, especially for the treatment of AF because of its selectivity for myocardial tissue ablation.[10,11,13] Representative pioneer researchers include but are not limited to Neven, Koruth, and Reddy et al. Neven delivered full-power electroporation ablation on anterior esophageal adventitia by using a linear suction device, and demonstrated that esophageal architecture remained unaffected 2 months after irreversible electroporation. Reddy and Koruth reported the first clinical experience of AF ablation with pulsed field ablation including epicardial and endocardial ablation.[11] However, electroporation ablation has been shown to create sufficiently large and deep lesions in or around pulmonary vein ostia for treatment of cardiac arrhythmias.[14] Whether these inevitable "lesions" will cause further damage to the esophageal wall, or even serious complications such as ulcers or perforations, needs further attention. This potential risk of NTIRE for esophageal damage needs to be sufficiently assessed under extreme ablation conditions, even reaching the level of tissue inactivation.

In this preliminary work, we chose to study the effect of NTIRE on the esophagus, which is often collaterally damaged during minimally invasive ablation procedures.[4,5,15,16] The main purpose is to clarify the esophageal histological changes after the whole layer ablation. Because of the ability of NTIRE to spare the extracellular matrix (ECM), it can be foreseeable that the esophagus will remain intact on the tissue scaffolds after ablation, and recover. We speculated that NTIRE should provide a safety and effectiveness profile and good subject tolerability.

METHODS

The data that support the findings of this study are available from the corresponding author upon reasonable request.

Grouping and In Vivo IRE Procedure

Eighty-four male, 6-month-old New Zealand rabbits with an average weight of 2.6±0.5 kg were used in this study. All animals received humane care and procedures were conducted under a protocol approved by the Ethics Committee of General Hospital of Northern Theater Command. All animal manipulations were conducted in accordance with national and international guidelines to minimize animal suffering. Animals were anesthetized by intramuscular injection with xylazine hydrochloride (5 mg/kg) and diazepam (0.5 mg/kg). The anterior approach of the neck was selected, and the middle of the incision was at the level of the second annular cartilage. A specially designed hand-held clamp, containing 2 parallel plate electrodes (Platinum Tweezertrode, 45-0486, BTX, USA), was applied across the targeted esophagus (Figure 1A). The measured distance between the 2 electrodes was ≈3.5 mm, which was consistent for all animals tested. By using an electroporation pulse generator (TP3032, Teslaman; Dalian, China), we delivered 9 trains of 10 direct current square pulses within electrode plates at 2000 V/cm with a pulse duration of 70 microseconds, a pulse interval of 100 milliseconds, and a train interval of 2 seconds (Figure 2). An oscilloscope trace of the voltage and current waveforms delivered were recorded to verify pulse delivery. The length of the esophageal ablation segment is ≈2 cm. The location of treatment was noted based on 2 suture knots, which were placed in the esophageal adventitia to mark the NTIRE-treatment region.

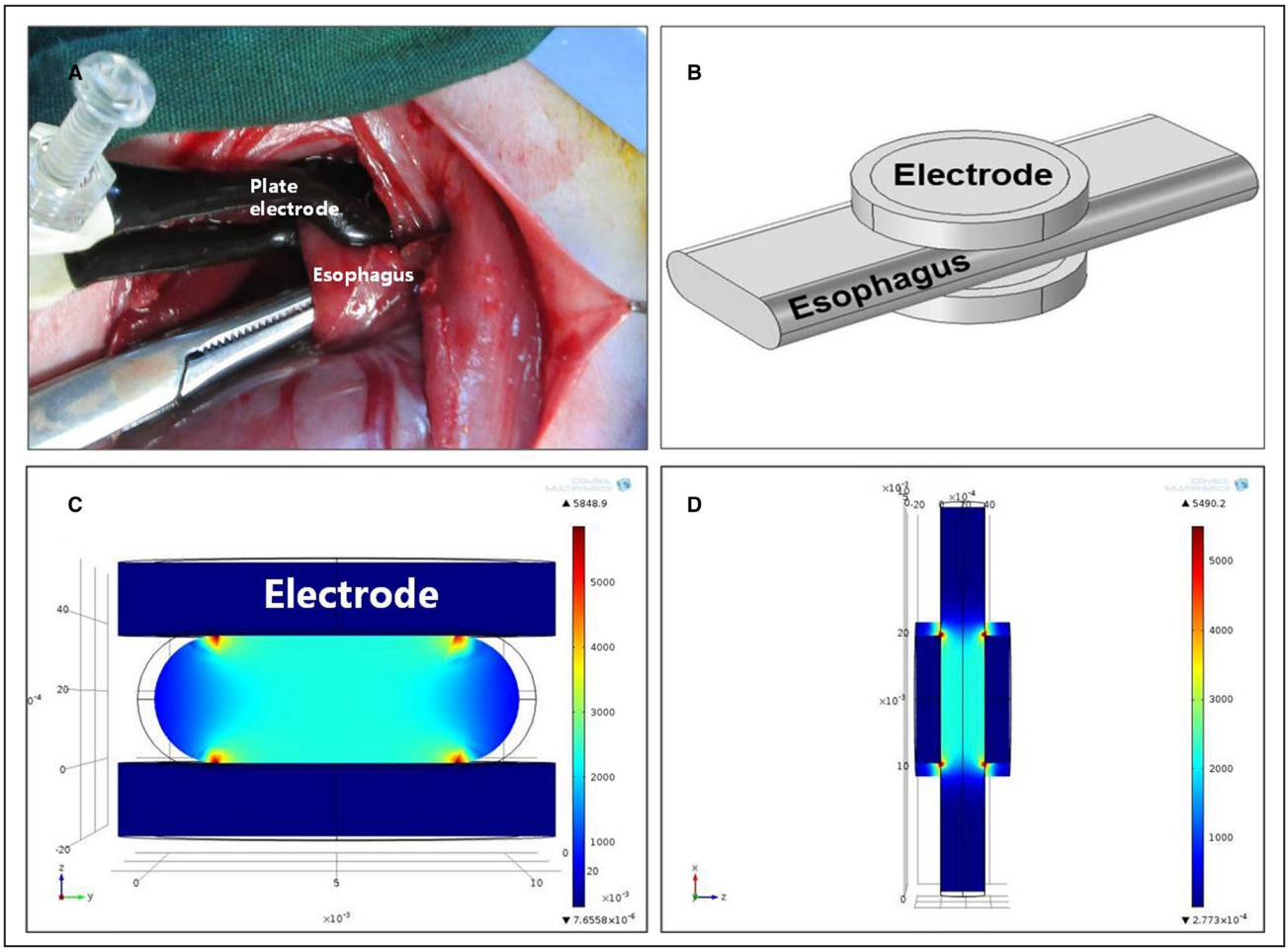

Figure 1. Esophagus ablation and electric field intensity distribution simulation.
A, Intraoperative picture of esophageal electroporation ablation. **B**, Three-dimensional simulation of esophagus clamped by 2 plate electrodes. **C**, Cross section of the ablation model. The electric field distribution between the 2 electrodes is substantially uniform. The highest electric field strengths appear at the edges of the electrodes (red areas), and the lowest strengths appear at the outer surface of the exposed esophageal wall between the 2 flat electrodes (dark blue areas). **D**, Longitudinal section of the ablation model.

Animals were divided into 22 groups, which contain 16 threshold parameter test groups (3 animals in each group) and 6 ablation groups (6 animals in each group). In each ablation group, 1 animal was selected as the random control and the electrode was only applied directly on its esophageal adventitia without pulse output, and all animals survived for 1, 3 days and 1, 2, 4, and 16 weeks before being euthanized. During the first 24 hours after surgery, the animals were given 2 additional doses of meperidine hydrochloride (1 mg/kg), spaced out over 8-hour increments. The animals were kept separately and carefully checked daily to ensure that they were not experiencing pain, stayed healthy, and recovered. Symptoms were monitored and an effort was made to relieve them. These symptoms included fever, reduced food intake and drinking, lack of locomotion, and swelling around the incision.

Determination of the Lowest Effective Ablation Threshold by Combination of Gradient Electric Field Intensity and Pulse Number

In each threshold parameter test group, in order to find the lowest effective ablation threshold, a combination of gradient electric field intensity and pulse number is used for verification. Four electric field intensities of 1000, 1500, 2000, and 2500 V/cm were selected, and 30, 60, 90, and 120 pulses were used for the corresponding ablation tests. Specimens were collected on day 3 postablation. Considering that the atrophy of muscle fibers after muscle cell death is more clearly visible in pathological sections, 5 regions of interest (ROI) (magnification ×40) were randomly selected from the cross-sectional muscle layer on each ablation section. The ratios between the numbers of atrophic muscle fibers to the total number of muscle fibers in

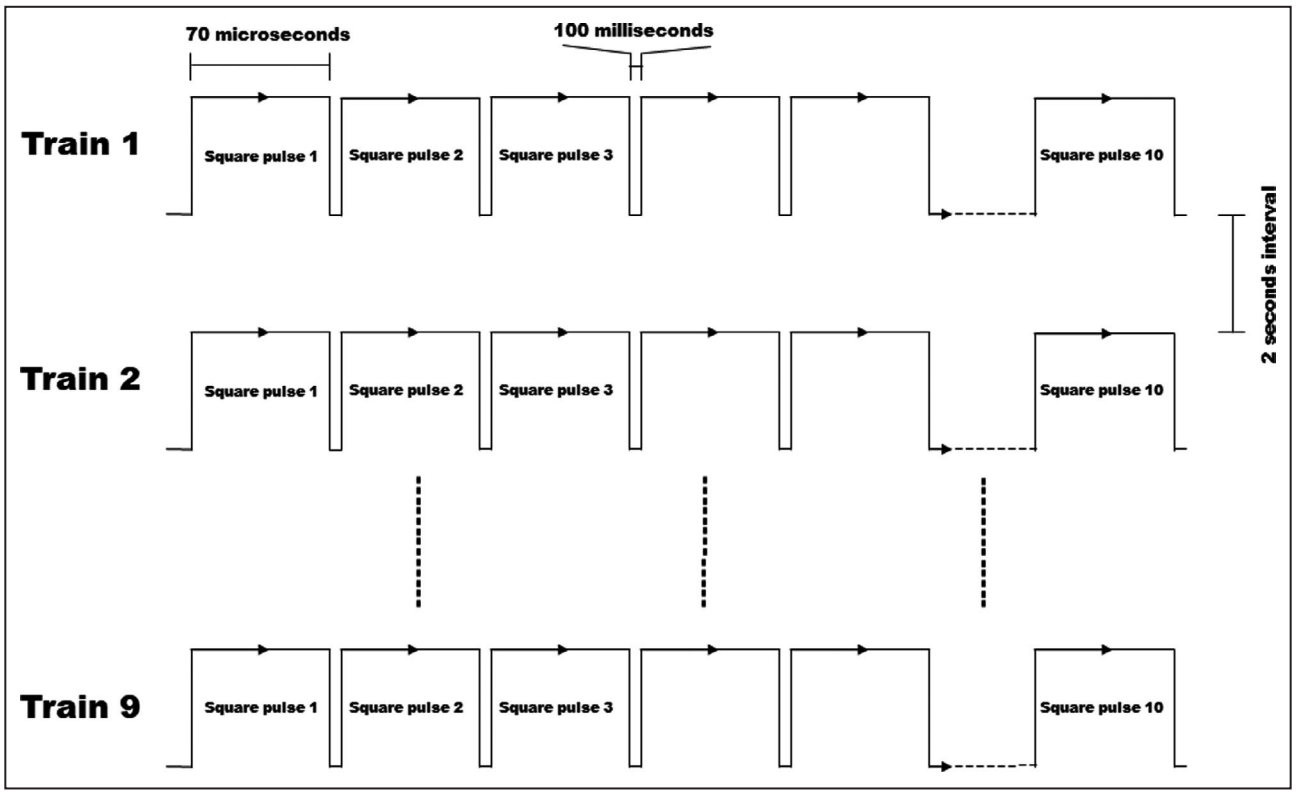

Figure 2. **Schematic diagram of the square wave pulses used in the experiment.**

the cross-sectional muscle fiber layers are shown in Figure 3.

Finite Element Modeling to Predict the Range of Effective Field Strength and Thermal Damage

In order to choose appropriate electrical parameters for experimental use that would induce complete tissue ablation while not causing extensive heating and thermal damage to the tissue, a transient finite element analysis was performed, modeling the electric field intensity distribution and the effect of Joule heating on the temperature distribution as described by Phillips et al.[8] A commercial finite element package (COMSOL Multiphysics 5.4) was used to develop the model and analyze the electrical treatment parameters. In this model, all tissues were considered homogeneous. The cross section of the esophagus was 2-dimensionally modeled as a runway shape (one 10×3.5-mm^2 rectangle and 2 semicircles with a diameter of 3.5 mm, as shown in Figure 1B) between 2 stainless steel electrodes (a circular plate with a diameter of 10 mm, and an insulating layer is attached to the outside of each metal electrode plate, as shown in Figure 1). The dimension of esophagus was based on experimental measurement. The dielectric measurements of esophageal tissue were performed 5 times on rabbit esophagus specimens previously, and the average±SD of multiple measurement results was set as the dielectric parameters for this experiment. The thermal and electrical properties of the esophagus were assumed to be both homogeneous and isotropic in cross-section. By using a signal analyzer (N9030A PXA; Agilent, USA), the conductivity values were 4.0e^6 [S/m] for the electrode, 1e^{-17} [S/m] for the insulating layer, and 0.97 [S/m] for the esophagus; the dielectric constants were 4.5 for the insulating layer and 4.0 for the esophagus. Electric field distribution in the tissue, caused by an electroporation pulse, was determined by solving the Laplace equation for static electric currents:[17]

$$\nabla(\sigma\nabla\varphi) = 0$$

where σ and φ are tissue electric conductivity and electric potential, respectively. The electrodes were modeled as an insulating body with an extension of stainless steel. The boundary conditions used in our calculations were a constant potential on the surface of the electrodes and electrical insulation on all outer boundaries of the model. In treatment planning, a numerical model of electroporation was used that did

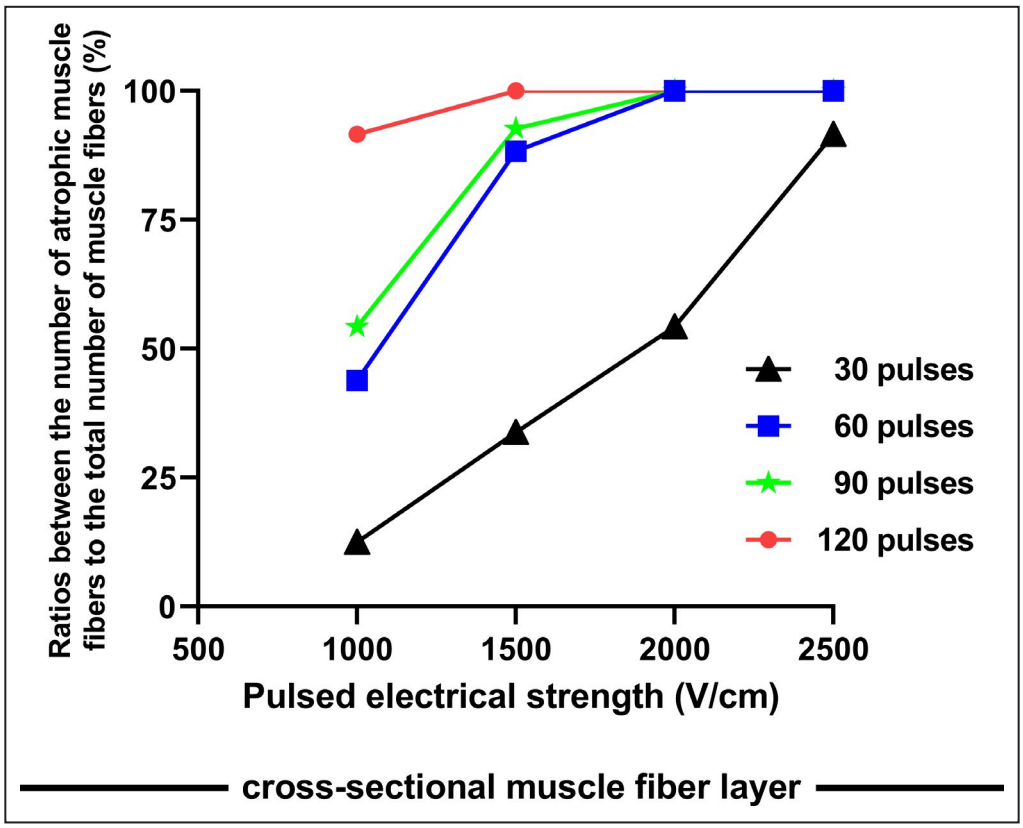

Figure 3. Ratios between the numbers of atrophic muscle fibers to the total number of muscle fibers in the cross-sectional muscle fiber layer.

not take into account changes in tissue conductivity during electroporation.

The thermal and electrical properties of the esophagus were assumed to be both isotropic and homogeneous in cross-section. This model followed the analysis described by Phillips et al.[18] Briefly, the Laplace equation was solved in order to determine the heat generation per unit volume caused by Joule heating (*qJH*):[17]

$$qJH = \sigma |\nabla \varphi|^2$$

The top electrode was set as having a positive potential (φ=Vo), and the bottom electrode was set as ground (φ=0), where Vo is the potential difference applied across the electrodes. The boundaries between the electrodes and air, and between the esophagus and air were set as electrically insulating.

Histological Examinations

The animals were weighed and euthanized with a mixture consisting of ketamine (150 mg/kg) and xylazine (20 mg/kg). The treated section, together with an untreated section of ≈1-cm long at both ends, were selected. Samples were immediately fixed with 10% buffered formalin, embedded in paraffin, and sectioned with a microtome (5-μm thick). Each sample was stained with hematoxylin and eosin to examine the basic morphological changes, and with Masson trichrome to examine the structure of the ECM. In Masson trichrome stain, collagen fibers were stained blue, muscle cells were stained reddish purple, and epithelial cells were stained light red or lilac.

Histological Data Measurement

The esophageal wall of control and ablated segment contained 3 layers: mucosa, submucosa, and muscle layer. Specific data for each layer of tissue were measured, collected, and are shown in Figure 4. Two ROIs were randomly selected in each specimen slice respectively (blue dotted square frame in Figure 5A). Each ROI was set as a square area, which was defined as: making a line segment along the surface of the esophageal mucosa (the length of the line segment is equal to the thickness of the esophageal wall); drawing a square at the position of the esophageal wall with the line segment as the side length; and taking the esophageal tissue contained by the square area as the ROI. We used Image-Pro Plus 6.0 software and took measurements in selected ROIs. The measurement results are displayed

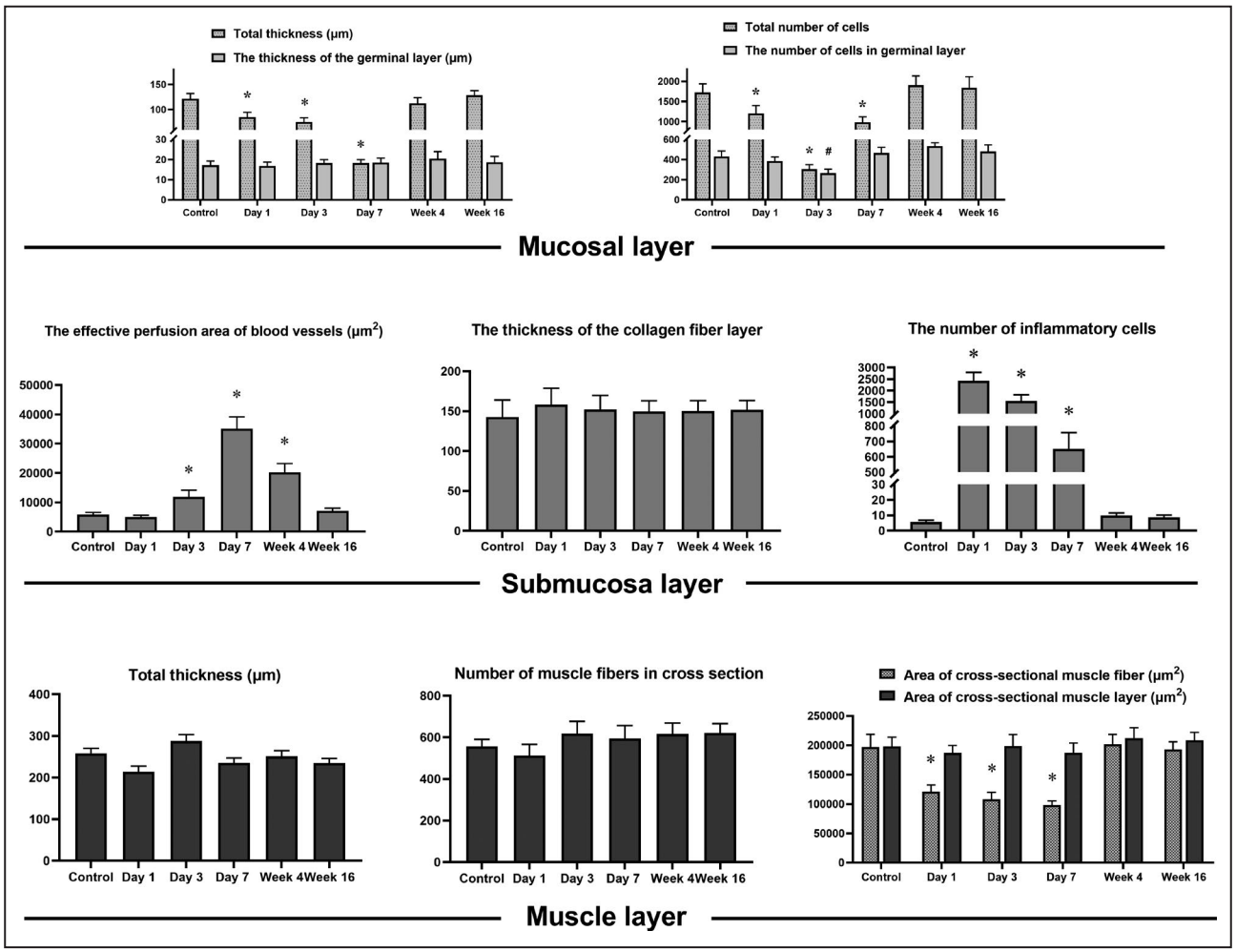

Figure 4. Histological data measurement of the esophageal wall after sham operation or nonthermal irreversible electroporation.
*/#$P<0.05$ compared with the normal control group.

as mean (SD). Specific measurement indicators are as follows: (In mucosal layer) the total thickness and the total number of cells, the thickness of the germinal layer and its number of cells; (in submucosa layer) the thickness, the effective perfusion area of blood vessels, the thickness of the collagen fiber layer (the Masson stained blue layer), and the number of inflammatory cells; (in muscle layer) the thickness, the number of muscle fibers in cross section, area of cross-sectional muscle fiber, and area of cross-sectional area.

Statistical Analysis

The observations are all independent, and do not result from repeated measures on each animal. Data are presented as the mean value±SD. One-way analysis of variance was used to evaluate differences among groups. The Dunnett *t* test was used for comparison between each experimental group and the control group. Differences between the means were considered significantly different when 2-sided *P* values were <0.05. All of the statistical analyses were performed using SPSS software (version 17.0, SPSS, Inc., Chicago, IL).

RESULTS

Determination of Effective Ablation Threshold

Compared with the decellularization of the mucosal layer and the muscle layer, atrophy of muscle fibers after muscle cell death is more clearly visible in pathological sections. Under the combination of different ablation parameters, we observed the ratios between the numbers of atrophic muscle fibers to the total number of muscle fibers in the cross-sectional muscle fibers layer. Data are shown in Figure 3. Measurement results show that the entire esophageal tissue can be completely inactivated

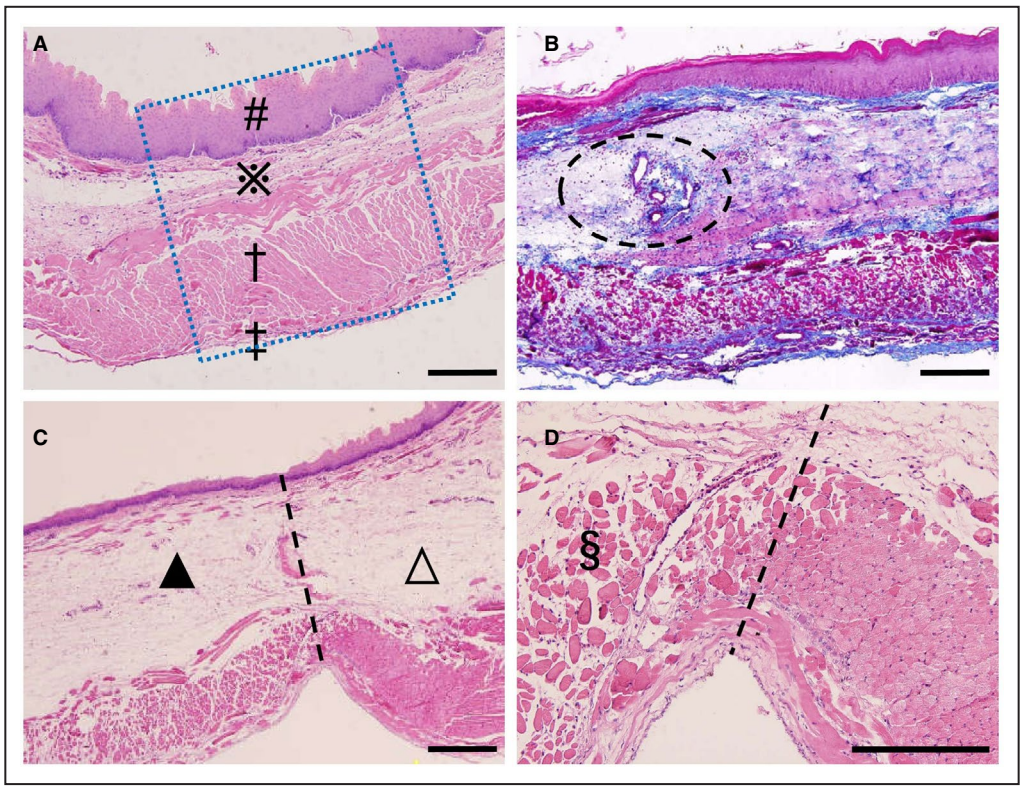

Figure 5. Tissue observation 1 day after esophageal ablation.
A, Untreated normal control. A typical healthy esophagus with mucosa (#), submucosa (※), muscular layer (†), and adventitia (‡) (The blue dotted square represents a region of interest). **B**, Ablation group with Masson trichrome staining. The fully retained collagen fiber framework is stained blue. Significant edema appears in the submucosa with a large number of inflammatory cell infiltrations. Small arteries and veins appear to be intact (dotted ellipse). **C**, Ablation group with hematoxylin and eosin staining. There is a clear boundary line between the nonthermal irreversible electroporation–treated area (▲) and the untreated area (Δ). The outer surface of the epithelial layer is partially exfoliated. **D**, A higher magnification of (**C**) shows completely ablated muscle layer, the dissolution and absorption of muscle cells, and the intact epimysium, perimysium, and endomysium (§). All bars represent 50 μm.

under the combination of 1500 V/cm field strength multiplied by 90 pulses. When the number of pulses remains unchanged while the field strength exceeds 1500 V/cm, or the field strength remains unchanged while the number of pulses is >90, or when the field strength and the number of pulses are both greater than the above reference value, the entire esophagus can be lethally ablated. In this study, we have chosen a parameter combination of 2000 V/cm multiplied by 90 pulses output, whose electric field strength is selected higher than the lowest effective threshold combination. The purpose is to see whether thermal damage will occur, and whether the ablated tissue will effectively regenerate and repair.

Distribution of the Electric Field Intensity and Prediction of Thermal Damage

Field strength modeling showed that the electric field distribution between the 2 plate electrodes was almost uniform when direct-current pulses of 2000 V/cm (voltage-to-distance ratio) were applied. Special field strengths include: the highest field intensity of 10 401 V/cm emerged at the edge of the electrode; and the lowest field intensity of 1150 V/cm emerged at the outer surface of the exposed esophageal wall between the 2 flat electrodes (Figure 1C and 1D).

The maximum tissue temperature obtained throughout the entire procedure was 40.21 °C, which is calculated by model simulation. This model showed very little temperature increase to the esophagus during the ablation procedure because the relatively large surface area of the stainless steel plate electrodes induced quick heat conduction to the electrodes and heat dissipation. Because this model predicts very little thermal damage while incorporating assumptions that would actually overpredict tissue temperature (overpredictions include ignoring a heat buffer system formed by blood flow in local tissue, ignoring heat loss caused by natural convection, and using the maximum tissue temperature to obtain the

damage parameter), it can be considered that the parameters modeled could be used experimentally without causing thermal damage to the esophagus in vivo.

Postablation Observation

One animal was lost during surgery because of an overdose of xylazine. Seven animals experienced mild anorexia after surgery and resolved on their own within 72 hours. Otherwise, the animals did not show any symptoms of typical pain, vomiting, weight loss, or melena. Direct visual inspection of the ablation area after NTIRE revealed no blood clots, and the inner surface of electrodes never showed signs of charring. Within a short time after ablation, the electrode plate caused slight congestion of small blood vessels and local vasodilation, and this phenomenon could last for 3 days. From day 3 to day 7 after ablation, no obvious lumen stenosis, epithelial erythema, erosions, or ulcerations were observed. From week 4 to week 16 after ablation, there were no macroscopic lesions on the esophageal epithelium and adventitia, and a gross specimen of the esophagus appeared normal.

Histopathological Assessment

Histological analysis of the esophagus was performed at 6 time points from day 1 to week 16 after ablation to examine the effects of NTIRE on the esophagus. The histology results represent only animal samples under 9 trains of 10 direct current square pulses of 2000 V/cm. According to Joule heating (qJH), it is believed that using a combination of parameters with electric field intensity and pulse number equal to or lower than this threshold will not cause additional thermal damage to the tissue.

On day 1, the boundary between the ablated and nonablated areas was clearly demarcated (Figure 5C and 5D). The selected irreversible electroporation protocol is strong enough to inactivate all layers of the esophagus. Acute inflammatory infiltration was observed throughout the entire layer of the esophagus wall. The superficial part of the epithelium exfoliated, but the basal epithelial layer was intact. The submucosa showed severe edema with a large number of inflammatory cell infiltrations, but the arterioles and veins were intact. The muscle layer was completely ablated, manifested by lysis of muscle cells and inflammatory infiltration of lymphocytes. There was no ischemia or injury such as pale mucosa, eschar, or perforation in gross specimen observation. Local temperature was not measured on histology, but it was inferred to be nonthermal based on the above nonthermal injury observation results. The basic tissue framework (such as collagen fibers) and structural details were well preserved throughout the esophageal wall. The connective tissues surrounding the striated muscle, bundles, and fibers are known as the epimysium, the perimysium, and the endomysium, respectively, which remained intact at this sampling time.

On day 3, the frame structure of the esophagus remained intact and there were no signs of lumen stenosis. The blood vessels, Meissner plexus, and regenerated muscle cells were clearly visible (Figure 6C). The structural details of the epithelium were preserved. The plica of esophagus, composed of the mucosa and submucosa, still maintained its original tissue structure and form. As indicated by the appearance of immature epithelial cells in the germinal layer of the epithelium, there were clear signs of mucosal regeneration and repair in the treated area. Meanwhile, immature muscle cells began to appear in the muscle layer.

On day 7, signs of tissue repair were evident (Figure 7). The most important features were an increase in the number of blood vessels in the submucosa, an expansion of the blood vessel lumen, and a rich blood supply. The esophagus appeared to have restored most of its structure and exhibited distinct

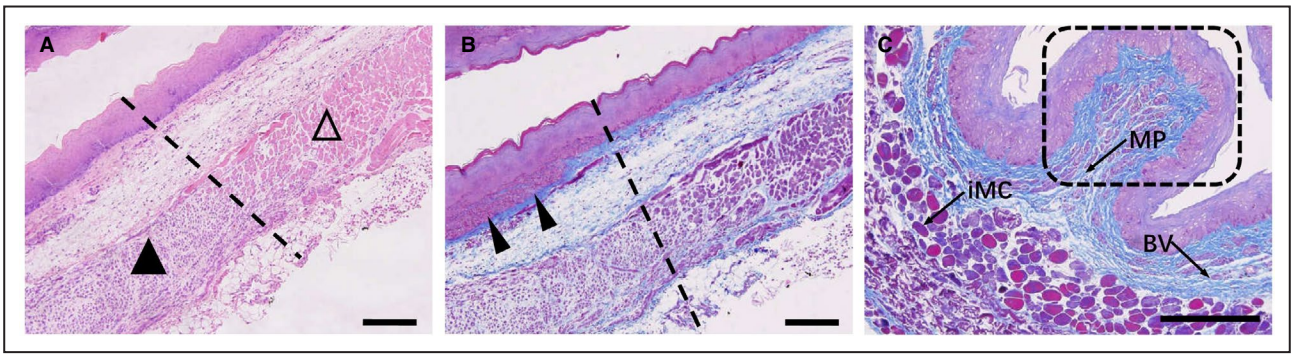

Figure 6. Tissue observation 3 days after esophageal ablation.
A, The interface between the nonthermal irreversible electroporation–treated region (▲) and untreated region (Δ). **B**, Immature epithelial cells appear in the basal layer of the mucosa (arrowheads), and regeneration and repair of the mucosa are vigorous. **C**, Masson trichrome staining shows that the plica, consisting of the mucosa and submucosa, still retains its primitive framework structure (dashed rectangle). The presence of blood vessels (BV), the Meissner plexus (MP), and immature muscle cells (iMC) can also be seen. All bars represent 50 μm.

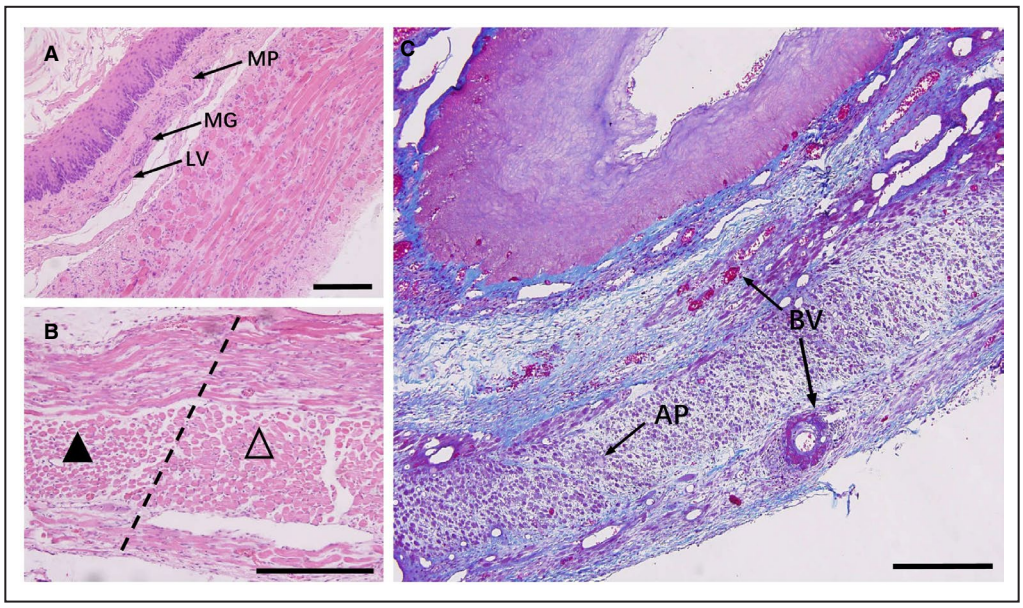

Figure 7. Tissue observation 7 days after esophageal ablation.
A, Distinct layers of tissue include a mucosal layer with nonkeratinized squamous epithelium, a submucosal layer containing mucus glands (MG), blood vessels (BV), lymphatic vessels (LV) and the Meissner plexus (MP), a muscular layer containing regular muscle fibers and rich Auerbach plexus, and a well-structured adventitia. B, In muscular layer, the interface between the nonthermal irreversible electroporation–treated region (▲) and the untreated region (Δ). C, Cross section of the esophagus stained with Masson trichrome. Signs of regeneration and repair appear: increased number of BV in the submucosa, dilation of the vascular lumen, an abundant blood supply, and well-ordered muscle fibers mixing with numerous Auerbach plexus (AP) and blood vessels. All bars represent 50 μm.

layers of tissue, including: a mucosal layer with nonkeratinized squamous epithelium, a submucosal layer containing mucus glands, blood vessels, lymphatic vessels and the Meissner plexus, a muscular layer containing regular muscle fibers and rich Auerbach plexus, and a well-structured adventitia.

From week 2, the epithelial surface began to keratinize, the epithelial basal cells were still vigorously proliferating, the submucosal vasodilatation was reduced, the muscle layer was clear, and the sarcoplasm of regenerated muscle cells tended to be full (Figure 8A). In our slice observation, the muscle layer of the esophagus is dominated by skeletal muscle cells, which is related to the sampling site of the esophagus. Of course, there were also some smooth muscle cells in between the collagen fibers and elastic fibers in submucosa, and in the luminal layer. Observed under the light microscope after ablation, these smooth muscle cells did not seem to have major changes in morphology, which is consistent with the study by Neven et al.[6]

From week 4 to week 16, esophageal repair and regeneration continued to improve, and its micromorphology gradually approached that of the normal control group (Figure 8B through 8D). The esophagus was not devascularized after NTIRE ablation; instead, the blood supply reached or even exceeded the levels of the normal control group at week 4, indicating that the vasculature was well preserved and blood vessel reconstruction was enhanced.

Histological Data Measurement and Statistical Analysis

As shown in Figure 4, histological data measurements of the esophagus were performed at the control group and 6 time points postablation in order to examine the effects of NTIRE on the esophagus.

In the mucosal layer: The total thickness of the mucosa decreased in the first 3 days after ablation, and reached the lowest value on day 3 ($P<0.05$), but no obvious change appeared in the thickness of the germinal layer. The number of cells either in the entire mucosa or in the germinal layer decreased gradually in the first 3 days, and decreased to the lowest point on day 3 ($P<0.05$); and then cell numbers gradually increased, and basically restored to the normal control group level at week 4.

In the submucosal layer: The effective vascular perfusion area increased significantly from day 3, and reached the highest value at day 7; and then gradually decreased, and finally restored to the normal control group level at week 16. The thickness

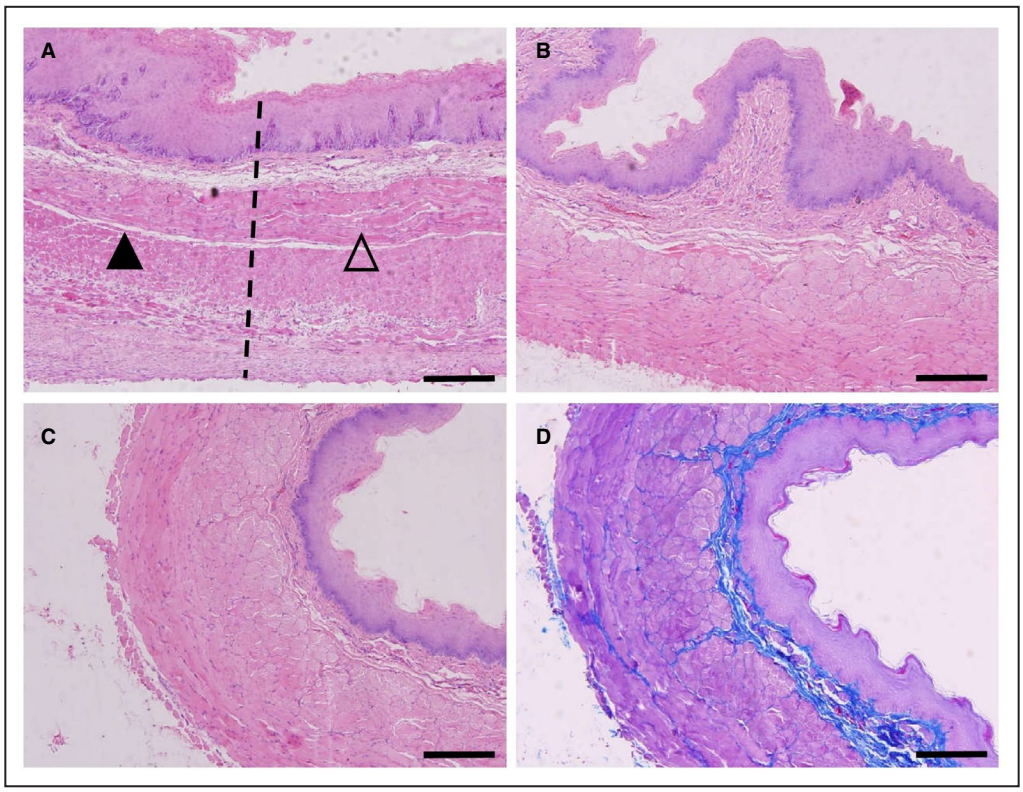

Figure 8. Midterm tissue observation after NTIRE ablation.
A, Two weeks post nonthermal irreversible electroporation (NTIRE). The interface between the treated region (▲) and the untreated region (Δ). The surface of the epithelium begins to keratinize, the epithelial basal cells still actively proliferate, the submucosal vasodilatation is reduced, the muscle layer is clear, and the sarcoplasm of regenerated muscle cells increases. **B**, Four weeks post NTIRE. A continuous improvement in repair and regeneration. **C**, Sixteen weeks post NTIRE. Microscopic morphology is close to that of the normal control group. **D**, Masson trichrome staining of (**C**). Blue staining shows a clear, continuous, and intact extracellular framework. All bars represent 50 μm.

of the collagen fiber layer (the Masson-stained blue layer) always remained stable. The number of inflammatory cells peaked on day 1, then gradually decreased, and restored to the control group level at week 4.

In the muscle layer: The total thickness, number of muscle fibers in cross section, and area of cross-sectional muscle layer remained the same from day 1 to week 16. The area of cross-sectional muscle fiber exhibited a gradual decrease trend shortly after ablation, dropped to the lowest point at day 7, and restored to the normal control group level at week 4.

DISCUSSION

This preliminary work indicates that NTIRE has the ability to preserve the ECM, important blood vessels, and nerve bundles. This feature allows for a quick recovery of the esophagus after electroporation ablation, and provides an important guarantee for the recovery of peristalsis and secretion of the esophagus.

NTIRE Ablation: Experimental Model and Parameter Selection

In order to understand the pathological changes of NTIRE to esophageal tissue more intuitively, we used a simple, basic, more direct NTIRE ablation parameter combination combining with a flat bipolar to carry out the study. In this cohort, ablation was performed in a monophasic-bipolar fashion using a classical NTIRE ablation system, which has been widely used in tissue ablation according to previous research. The ablation waveforms, which were similar to or not lower than the electric field strengths used in endocardial ablation or epicardial ablation,[9–12] consisted of a sequence of microsecond scale square pulses at 2000 V/cm. Our research team has used this similar combination parameter in animals to prove that it reaches to lethal ablation on bone, tendon, peripheral nerve, and skeletal muscle, while the ablated tissue can repair and regenerate in follow-up observation.[19–21] Although this approach cannot be completely equivalent to test catheters designed for endocardial delivery of the

more modern biphasic pulsed-field ablation waveforms being studied preclinically and clinically, it fully encompasses the entire esophagus between plate electrodes, which could be considered a worst-case scenario because of a relatively uniform electric field intensity distribution. Therefore, the research results will help determine the NTIRE parameter threshold for histopathological damage of the esophagus, optimize the parameter combination scheme, and avoid unnecessary tissue damage in advance.

In this study, through the gradient parameter combination test, we confirm that 1500 V/cm multiplied by 90 pulses is an effective ablation threshold of esophageal tissue. Combining through finite element calculations, we find that when a field strength of 1500 V/cm is applied, the local tissue can be completely inactivated, even tissue at the point of lowest electric field strength. The ideal combination of parameters can ensure effective tissue ablation without excessively increasing the risk of tissue thermal damage. Therefore, a parameter combination that is equal to or higher than the above pairing parameters may be appropriate. The actual electric field strength used in this study is higher than the field strength of the lowest efficient ablation threshold. By using finite element modeling, we have ensured that the parameters used are able to complete effective ablation without unnecessary thermal damage caused by Joule heat.

Efficacy of NTIRE Ablation

It is reported that NTIRE ablation can inactivate targeted cells while retaining tissue scaffolds.[22] The structural integrity of vessels and nerves remains intact, and the retention of collagen scaffold allows subsequent tissue repair and regeneration.[7] Through the experiment, all cells in the entire layer of the esophagus wall were completely ablated at day 1 postablation, and signs of recovery began to appear after 3 days, which indicates that the applied electrical parameters are strong enough to cause irreversible electroporation in all layers of tissue without generating excessive thermal damage.

We observe that the esophagus undergoes 3 characteristic stages after NTIRE, each of which has its own unique histological manifestations and biological significance. The first stage is the period of tissue ablation, including cell death, tissue edema, inflammatory infiltration, and decellularization. Because of complete ablation of the mucosal, submucosal and muscular layers, NTIRE-induced cell death occurs quickly. Partial exfoliation occurred in the epithelial layer, and the muscular structure details in the muscle layer were completely lost. The second stage is the cell regeneration phase, including the phase of cell regeneration, proliferation, and tissue revascularization. NTIRE specifically targets the cell membrane, allowing for the preservation of tissue structural components such as the ECM, blood vessels, and nerve fibers.[18] This holds true for the esophagus as well. The necessary microenvironment after NTIRE ablation offers the possibility of rapid regeneration and proliferation of tissue cells. On day 1 and day 3 postablation, Masson trichrome staining showed that the ECM was still intact, and the nerves, lymph vessels, and blood vessels were still functioning, providing a necessary functional framework for epithelialization and muscle cell regeneration. Although the observed ECM edema may cause tissue ischemia in the ablation segment on day 3, subsequent observations showed that the blood supply was fully restored or even increased. One week after ablation, signs of tissue repair were already evident. Previous studies have shown that the epithelial lamina propria of the esophagus contains multipotent stem cells, which differentiate and mature gradually, replacing cells that slough off in normal, healthy tissue every 1 to 3 days.[23] Though the epithelial cells within the treated region were ablated, it appeared that immature epithelial cells or lamina propria–derived stem cells were being produced from the edges of the treated regions, and were able to migrate inward to the treated region and produce a new epithelial cell layer. The third stage is the period of tissue remodeling, including remodeling of ablated tissue and complete recovery of the blood supply. It should be noted that “regeneration” in this study refers to the restoration of the tissue morphology after ablation to a state indistinguishable from the control group observed under an optical microscope, but does not include the restoration or change of the functional state of the tissue (eg, does not include nerve electrophysiological activity of esophageal tissue). What needs to be pointed out is that the complete regeneration seen in this protocol is neither unique to the pulse sequence used in this study nor unique to the animal model itself. NTIRE’s ability to retain the tissue framework will greatly aid in the overall recovery of the esophagus. The framework structure such as the epimysium and the perimysium, which are mainly composed of reticular collagen fibers and elastic fibers, remained intact after NTIRE. Thermal coagulation and thrombosis to the blood vessels has not occurred, and the capillaries are open and blood is flowing. Neven et al used a porcine model to study the acute and long-term effects of electroporation ablation on the esophagus and found small scar formation.[6] They completed a good preclinical study; but Koruth et al and our team did not find signs of tissue fibrosis. We believe these 2 independent studies may differ in the following aspects: (1) the number of inflammatory cells, and the degree and duration of inflammatory response; (2) the number of fibroblasts and cell activity, and the effectiveness of fibroblasts to make collagen fibers; (3) differences in animal species; and (4) the number of

tissue stem cells and their directed differentiation ability. Although long-term studies are needed to determine what effect NTIRE will have on the esophagus years after treatment, it is believed that the unique ability of NTIRE to retain blood vessels and the ECM not only helps tissue recover in the short term after ablation, but could also protect the tissue from developing long-term complications in thermal ablation treatments.

Several unique characteristics distinguish NTIRE from current thermal ablation techniques. First, under the premise that the conductivity remains unchanged, the Joule heating is directly related to electric field strength, and NTIRE is not associated with a temperature increase or with protein denaturation if not in a sufficiently strong field[24]; rather, it effectively retains the protein activity, which plays an inductive role during tissue regeneration.[25] Second, NTIRE causes complete tissue ablation partially through apoptosis, pyroptosis, or "apoptosis-mimetic" necrosis (known as necroptosis).[26] There is emerging evidence that apoptotic cells release growth signals, stimulate the proliferation of progenitor or stem cells, and promote tissue regeneration.[27] Cell death following NTIRE treatment activates the local innate immune system, which shifts the microenvironment from an anti-inflammatory state to a pro-inflammatory state. The nonthermal damage to increased innate immune system stimulation improves antigen presentation, resulting in the engagement of the adaptive immune system. Third, NTIRE might have a unique ability to spare critical structures, including collagen fibers and the blood vessels.[28] It can be predicted that if some thermal ablation methods were applied to the esophagus, they would cause severe lumen stenosis. Instead, effective maintenance of overall framework tissue integrity and reduced fibrosis have been reported as favorable side effects of NTIRE in comparison to other thermal ablation methods.[29] It is evident that the intact vascular preservation is fundamental for both necrotic tissue resorption and in situ tissue regeneration.

This study carries out esophageal tolerance research about in situ electroporation ablation. The purpose of the study is to offer a transition bridge from experimental research to clinical application and to establish a safety guarantee for para-esophageal electroporation. The esophageal tissue passively undergoing ablation after being covered by a pulsed electric field retains the basic material conditions for tissue repair and regeneration, which would at least not have serious lethal complications such as fistula formation or esophageal perforation.

Study Limitations

Although this study attests to the relative esophageal-sparing effects of NTIRE, the approach used in this study is still fundamentally different from the exposure human esophagus would endure during left atrial ablation. The approach cannot be simply applied to test catheters designed for endocardial delivery of the more modern biphasic pulsed field ablation waveforms being studied preclinically and clinically. Further studies should be performed to carry out research in large animals to make the research results closer to those for humans. The use of numerical models will also provide great advantages for the progression of NTIRE cardiac ablation to human clinical trials, reducing inefficiency and cost of long-term preclinical trials. Meeting these issues will bring NTIRE ablation 1 step closer to in-human studies.

CONCLUSIONS

Monophasic, bipolar NTIRE delivered using the plate electrodes in a novel esophageal injury model demonstrates no histopathologic changes to the esophagus at 16 weeks. Data of this study suggest that electroporation ablation is a safe modality for pulsed electroporation ablation near the esophagus.

ARTICLE INFORMATION

Received March 11, 2021; accepted August 18, 2021.

Affiliations

Department of Urology (Y.S., L.F.) and Department of Anesthesia, General Hospital of Northern Theater Command, Shenyang, China (J.Z.).

Acknowledgments

We would like to thank Dr Zhao Li (Yuncheng Central Hospital, Shanxi, China) and Qiang Lu (Tangdu Hospital, Air Force Medical University, Shaanxi, China) for the surgical and anatomical technical support for experimental animals. YS and JJZ supervised the study and designed experiments, and YS, LHF, and JJZ executed experiments and analyzed data.

Sources of Funding

This study was funded by the Natural Science Foundation of Liaoning Province (2019-MS-003), the National Natural Science Foundation of China (81801878), and the Medical Youth Development Program of the PLA (20QNPY089).

Disclosures

We declare that there are no financial conflicts of interest to disclose.

REFERENCES

1. Andersson T, Magnuson A, Bryngelsson IL, Frobert O, Henriksson KM, Edvardsson N, Poci D. All-cause mortality in 272,186 patients hospitalized with incident atrial fibrillation 1995–2008: a Swedish nationwide long-term case-control study. *Eur Heart J*. 2013;34:1061–1067. doi: 10.1093/eurheartj/ehs469
2. Wolf PA, Abbott RD, Kannel WB. Atrial fibrillation as an independent risk factor for stroke: the Framingham Study. *Stroke*. 1991;22:983–988. doi: 10.1161/01.STR.22.8.983
3. Wojtaszczyk A, Caluori G, Pesl M, Melajova K, Starek Z. Irreversible electroporation ablation for atrial fibrillation. *J Cardiovasc Electrophysiol*. 2018;29:643–651. doi: 10.1111/jce.13454
4. Pappone C, Oral H, Santinelli V, Vicedomini G, Lang CC, Manguso F, Torracca L, Benussi S, Alfieri O, Hong R, et al. Atrio-esophageal fistula

as a complication of percutaneous transcatheter ablation of atrial fibrillation. *Circulation*. 2004;109:2724–2726. doi: 10.1161/01.CIR.0000131866.44650.46
5. Schmidt B, Metzner A, Chun KR, Leftheriotis D, Yoshiga Y, Fuernkranz A, Neven K, Tilz RR, Wissner E, Ouyang F, et al. Feasibility of circumferential pulmonary vein isolation using a novel endoscopic ablation system. *Circ Arrhythm Electrophysiol*. 2010;3:481–488. doi: 10.1161/CIRCEP.110.954149
6. Neven K, van Es R, van Driel V, van Wessel H, Fidder H, Vink A, Doevendans P, Wittkampf F. Acute and long-term effects of full-power electroporation ablation directly on the porcine esophagus. *Circ Arrhythm Electrophysiol*. 2017;10:e004672. doi: 10.1161/CIRCEP.116.004672
7. Schoellnast H, Monette S, Ezell PC, Deodhar A, Maybody M, Erinjeri JP, Stubblefield MD, Single GW Jr, Hamilton WC Jr, Solomon SB. Acute and subacute effects of irreversible electroporation on nerves: experimental study in a pig model. *Radiology*. 2011;260:421–427. doi: 10.1148/radiol.11103505
8. Phillips MA, Narayan R, Padath T, Rubinsky B. Irreversible electroporation on the small intestine. *Br J Cancer*. 2012;106:490–495. doi: 10.1038/bjc.2011.582
9. Koruth J, Kuroki K, Iwasawa J, Enomoto Y, Viswanathan R, Brose R, Buck ED, Speltz M, Dukkipati SR, Reddy VY. Preclinical evaluation of pulsed field ablation: electrophysiological and histological assessment of thoracic vein isolation. *Circ Arrhythm Electrophysiol*. 2019;12:e007781. doi: 10.1161/CIRCEP.119.007781
10. Reddy VY, Neuzil P, Koruth JS, Petru J, Funosako M, Cochet H, Sediva L, Chovanec M, Dukkipati SR, Jais P. Pulsed field ablation for pulmonary vein isolation in atrial fibrillation. *J Am Coll Cardiol*. 2019;74:315–326. doi: 10.1016/j.jacc.2019.04.021
11. , Koruth J, Jais P, Petru J, Timko F, Skalsky I, Hebeler R, Labrousse L, Barandon L, Kralovec S, et al. Ablation of atrial fibrillation with pulsed electric fields: an ultra-rapid, tissue-selective modality for cardiac ablation. *JACC Clin Electrophysiol*. 2018;4:987–995. doi: 10.1016/j.jacep.2018.04.005
12. Koruth JS, Kuroki K, Kawamura I, Brose R, Viswanathan R, Buck ED, Donskoy E, Neuzil P, Dukkipati SR, Reddy VY. Pulsed field ablation versus radiofrequency ablation: esophageal injury in a novel porcine model. *Circ Arrhythm Electrophysiol*. 2020;13:e008303. doi: 10.1161/CIRCEP.119.008303
13. Bhardwaj R, Koruth JS. Novel ablation approaches for challenging atrial fibrillation cases (mapping, irrigation, and catheters). *Cardiol Clin*. 2019;37:207–219. doi: 10.1016/j.ccl.2019.01.012
14. Wittkampf FH, van Driel VJ, van Wessel H, Neven KG, Grundeman PF, Vink A, Loh P, Doevendans PA. Myocardial lesion depth with circular electroporation ablation. *Circ Arrhythm Electrophysiol*. 2012;5:581–586. doi: 10.1161/CIRCEP.111.970079
15. Stockigt F, Schrickel JW, Andrie R, Lickfett L. Atrioesophageal fistula after cryoballoon pulmonary vein isolation. *J Cardiovasc Electrophysiol*. 2012;23:1254–1257. doi: 10.1111/j.1540-8167.2012.02324.x
16. Deneke T, Schade A, Diegeler A, Nentwich K. Esophago-pericardial fistula complicating atrial fibrillation ablation using a novel irrigated radiofrequency multipolar ablation catheter. *J Cardiovasc Electrophysiol*. 2014;25:442–443. doi: 10.1111/jce.12308
17. Sersa G, Miklavcic D, Cemazar M, Rudolf Z, Pucihar G, Snoj M. Electrochemotherapy in treatment of tumours. *Eur J Surg Oncol*. 2008;34:232–240. doi: 10.1016/j.ejso.2007.05.016
18. Phillips M, Maor E, Rubinsky B. Nonthermal irreversible electroporation for tissue decellularization. *J Biomech Eng*. 2010;132:091003. doi: 10.1115/1.4001882
19. Song Y, Zheng J, Yan M, Ding W, Xu K, Fan Q, Li Z. The effect of irreversible electroporation on the femur: experimental study in a rabbit model. *Sci Rep*. 2015;5:18187. doi: 10.1038/srep18187
20. Song Y, Zheng J, Yan M, Ding W, Xu K, Fan Q, Li Z. The effects of irreversible electroporation on the achilles tendon: an experimental study in a rabbit model. *PLoS One*. 2015;10:e0131404. doi: 10.1371/journal.pone.0131404
21. Li W, Fan Q, Ji Z, Qiu X, Li Z. The effects of irreversible electroporation (IRE) on nerves. *PLoS One*. 2011;6:e18831. doi: 10.1371/journal.pone.0018831
22. Ball C, Thomson KR, Kavnoudias H. Irreversible electroporation: a new challenge in "out of operating theater" anesthesia. *Anesth Analg*. 2010;110:1305–1309. doi: 10.1213/ANE.0b013e3181d27b30
23. Islam F, Gopalan V, Wahab R, Smith RA, Lam AK. Cancer stem cells in oesophageal squamous cell carcinoma: identification, prognostic and treatment perspectives. *Crit Rev Oncol Hematol*. 2015;96:9–19. doi: 10.1016/j.critrevonc.2015.04.007
24. Yarmush ML, Golberg A, Sersa G, Kotnik T, Miklavcic D. Electroporation-based technologies for medicine: principles, applications, and challenges. *Annu Rev Biomed Eng*. 2014;16:295–320. doi: 10.1146/annurev-bioeng-071813-104622
25. Kawai M, Kataoka Y, Sonobe J, Yamamoto H, Maruyama H, Yamamoto T, Bessho K, Ohura K. Analysis of mineral apposition rates during alveolar bone regeneration over three weeks following transfer of BMP-2/7 gene via in vivo electroporation. *Eur J Histochem*. 2018;62. doi: 10.4081/ejh.2018.2947
26. Zhang Y, Lyu C, Liu Y, Lv Y, Chang TT, Rubinsky B. Molecular and histological study on the effects of non-thermal irreversible electroporation on the liver. *Biochem Biophys Res Commun*. 2018;500:665–670. doi: 10.1016/j.bbrc.2018.04.132
27. Brecht K, Weigert A, Hu J, Popp R, Fisslthaler B, Korff T, Fleming I, Geisslinger G, Brune B. Macrophages programmed by apoptotic cells promote angiogenesis via prostaglandin E2. *FASEB J*. 2011;25:2408–2417.
28. Scheffer HJ, Nielsen K, de Jong MC, van Tilborg AA, Vieveen JM, Bouwman AR, Meijer S, van Kuijk C, van den Tol PM, Meijerink MR. Irreversible electroporation for nonthermal tumor ablation in the clinical setting: a systematic review of safety and efficacy. *J Vasc Interv Radiol*. 2014;25:997–1011. quiz 1011. doi: 10.1016/j.jvir.2014.01.028
29. Golberg A, Broelsch GF, Bohr S, Mihm MC Jr, Austen WG Jr, Albadawi H, Watkins MT, Yarmush ML. Non-thermal, pulsed electric field cell ablation: a novel tool for regenerative medicine and scarless skin regeneration. *Technology*. 2013;1:1–8. doi: 10.1142/S233954781320001X